ELECTRONIC SUPPORTING INFORMATION

Concomitant Conformational Dimorphism in 1,2-Bis(9-anthryl)acetylene

Rebecca I. Goldstein,[a] Rui Guo,[b] Conor Hughes,[a] Daniel P. Maurer,[a] Timothy R. Newhouse,[a] Thomas J. Sisto,[a] Rebecca R. Conry,[a*] Sarah L. Price,[b*] and Dasan M. Thamattoor[a*]

[a]Department of Chemistry, Colby College, Waterville, ME 04901 USA; rrconry@colby.edu (RRC); dmthamat@colby.edu (DMT)
[b]Department of Chemistry, University College London, 20 Gordon Street, London WC1H 0AJ, United Kingdom. s.l.price@ucl.ac.uk (SLP)

TABLE OF CONTENTS

Details of X-ray Diffraction Experiments

X-ray data were collected at 173 K for both polymorphs, **1α** and **1β**, on a Bruker Smart Apex CCD diffractometer using a graphite monochromator and Mo Kα radiation (λ = 0.71073 Å). All data were processed with the Bruker Apex2 suite of programs.[1] The frames were integrated with the Bruker SAINT software package using a narrow-frame algorithm[2] and data were corrected for absorption effects using the multi-scan method (SADABS).[3] The structures were solved by direct methods, and refined by full-matrix least-squares on F^2, using the Bruker SHELXTL software package.[4] All nonhydrogen atoms were refined anisotropically and the hydrogen atoms were calculated using a riding model. The software program enCIFer[5] was used in conjunction with the checkCIF/Platon facility of IUCr to validate cif files.

Polymorph 1α:[6] This is the quasi-planar conformer whose structure has been reported before.[7] An orange-red needle-like specimen of approximate dimensions 0.06 mm x 0.06 mm x 0.46 mm, was used for the X-ray crystallographic analysis. The total exposure time was 23.11 hours. The integration of the data using a monoclinic unit cell yielded a total of 7288 reflections to a maximum θ angle of 26.22° (0.80 Å resolution), of which 1907 were independent (average redundancy 3.822, completeness = 99.7%, R_{int} = 2.74%, R_{sig} = 2.54%) and 1217 (63.82%) were greater than $2\sigma(F^2)$. The final cell constants of a = 12.388(3) Å, b = 5.0693(11) Å, c = 15.112(3) Å, β = 94.269(3)°, volume = 946.4(4) $Å^3$, are based upon the refinement of the XYZ-centroids of 1134 reflections above 20 σ(I) with 5.406° < 2θ < 50.20°. The ratio of minimum to maximum apparent transmission was 0.879. The calculated minimum and maximum transmission coefficients (based on crystal size) are 0.9660 and 0.9950.
The final anisotropic full-matrix least-squares refinement on F^2 with 136 variables converged at R1 = 5.30%, for the observed data and wR2 = 15.95% for all data. The goodness-of-fit was 1.013. The largest peak in the final difference electron density synthesis was 0.264 e-/$Å^3$ and the largest hole was -0.134 e-/$Å^3$ with an RMS deviation of 0.047 e-/$Å^3$. On the basis of the final model, the calculated density was 1.328 g/cm^3 and F(000), 396 e-.

Polymorph 1β:[8] This corresponds to the new, twisted polymorph. A light yellow block-like specimen of approximate dimensions 0.10 mm x 0.15 mm x 0.18 mm, was used for the X-ray crystallographic analysis. The total exposure time was 15.41 hours. The integration of the data using a monoclinic unit cell yielded a total of 8566 reflections to a maximum θ angle of 27.12° (0.78 Å resolution), of which 2147 were independent (average redundancy 3.990, completeness = 100.0%, R_{int} = 1.81%, R_{sig} = 1.58%) and 1637 (76.20%) were greater than $2\sigma(F^2)$. The final cell constants of a = 12.8185(10) Å, b = 14.0656(11) Å, c = 11.5956(9) Å, β = 112.1330(10)°, volume = 1936.6(3) $Å^3$, are based upon the refinement of the XYZ-centroids of 2441 reflections above 20 σ(I) with 4.489° < 2θ < 54.04°. The ratio of minimum to maximum apparent transmission was 0.901. The calculated minimum and maximum transmission coefficients (based on crystal size) are 0.9870 and 0.9930.
The final anisotropic full-matrix least-squares refinement on F^2 with 136 variables converged at R1 = 4.85%, for the observed data and wR2 = 15.30% for all data. The goodness-of-fit was 1.060. The largest peak in the final difference electron density

synthesis was 0.259 e-/Å^3 and the largest hole was -0.179 e-/Å^3 with an RMS deviation of 0.043 e-/Å^3. On the basis of the final model, the calculated density was 1.298 g/cm^3 and F(000), 792 e-.

References:

1. APEX2 (version 2014.5); Bruker AXS Inc., Madison, Wisconsin, USA.
2. SAINT (Version 8.34A); Bruker AXS Inc., Madison, Wisconsin, USA.
3. SADABS (Version 2014/2); G. M. Sheldrick, University of Gottingen, Germany; Bruker AXS Inc. Madison, Wisconsin, USA.
4. (a) XPREP (Version 2013/3); XS (Version 2013/1); XL (Version 2013/3); G. M. Sheldrick, University of Gottingen, Germany; Bruker AXS Inc. Madison, Wisconsin, USA. (b) G. M. Sheldrick, Acta Cryst., 2008, A64, 112.
5. F. H. Allen, O. Johnson, G. P. Shields, B. R. Smith and M. Towler, *J. Appl. Crystallogr.*, 2004, **37**, 335.
6. CCDC XXXXXXX contains supplementary crystallographic data for this polymorph.
7. (a) L. Jiang, J. Gao, E. Wang, H. Li, Z. Wang, W. Hu and L. Jiang, *Adv. Mater.*, 2008, **20**, 2735. (b) H. D. Becker, B. W. Skelton and A. H. White, *Aust. J. Chem.*, 1985, **38**, 1567.
8. CCDC 1036772 contains supplementary crystallographic data for this polymorph.

Table 1. Sample and crystal data for 1α.

Identification code	DT1477 CCDC **1059941**	
Chemical formula	$C_{30}H_{18}$	
Formula weight	378.44 g/mol	
Temperature	173(2) K	
Wavelength	0.71073 Å	
Crystal size	0.060 x 0.060 x 0.460 mm	
Crystal system	monoclinic	
Space group	P 1 21/n 1	
Unit cell dimensions	a = 12.388(3) Å	α = 90°
	b = 5.0693(11) Å	β = 94.269(3)°
	c = 15.112(3) Å	γ = 90°
Volume	946.4(4) $Å^3$	
Z	2	
Density (calculated)	1.328 g/cm^3	
Absorption coefficient	0.075 mm^{-1}	
F(000)	396	

Table 2. Data collection and structure refinement for 1α.

Theta range for data collection	2.05 to 26.22°	
Index ranges	-14<=h<=15, -6<=k<=6, -18<=l<=18	
Reflections collected	7288	
Independent reflections	1907 [R(int) = 0.0274]	
Coverage of independent reflections	99.7%	
Absorption correction	multi-scan	
Max. and min. transmission	0.9950 and 0.9660	
Refinement method	Full-matrix least-squares on F^2	
Refinement program	SHELXL-2014/6 (Sheldrick, 2014)	
Function minimized	$\Sigma\, w(F_o^2 - F_c^2)^2$	
Data / restraints / parameters	1907 / 0 / 136	
Goodness-of-fit on F^2	1.013	
Final R indices	1217 data; I>2σ(I)	R1 = 0.0530, wR2 = 0.1340
	all data	R1 = 0.0825, wR2 = 0.1595
Weighting scheme	$w=1/[\sigma^2(F_o^2)+(0.0909P)^2+0.0020P]$ where $P=(F_o^2+2F_c^2)/3$	
Largest diff. peak and hole	0.264 and -0.134 $eÅ^{-3}$	
R.M.S. deviation from mean	0.047 $eÅ^{-3}$	

Table 3. Atomic coordinates and equivalent isotropic atomic displacement parameters (Å²) for 1α.

U(eq) is defined as one third of the trace of the orthogonalized U_{ij} tensor.

	x/a	y/b	z/c	U(eq)
C1	0.93427(13)	0.2087(3)	0.42073(10)	0.0357(4)
C2	0.98884(13)	0.1202(3)	0.34739(10)	0.0374(4)
C3	0.08728(15)	0.2342(3)	0.32376(11)	0.0454(5)
C4	0.13716(16)	0.1481(4)	0.25205(12)	0.0517(5)
C5	0.09301(16)	0.9376(3)	0.19941(12)	0.0518(5)
C6	0.99996(15)	0.8216(3)	0.21969(12)	0.0473(5)
C7	0.94383(14)	0.9081(3)	0.29346(11)	0.0400(4)
C8	0.84657(14)	0.7945(3)	0.31371(11)	0.0432(5)
C9	0.79032(14)	0.8816(3)	0.38450(11)	0.0404(4)
C10	0.68973(15)	0.7673(3)	0.40382(12)	0.0481(5)
C11	0.63535(15)	0.8542(4)	0.47220(12)	0.0528(5)
C12	0.67784(16)	0.0625(3)	0.52657(12)	0.0526(5)
C13	0.77396(14)	0.1764(3)	0.51072(11)	0.0459(5)
C14	0.83413(13)	0.0926(3)	0.43947(10)	0.0378(4)
C15	0.98034(13)	0.4141(3)	0.47657(10)	0.0386(4)

Table 4. Bond lengths (Å) for 1α.

C1-C2	1.414(2)	C1-C14	1.420(2)
C1-C15	1.432(2)	C2-C3	1.419(2)
C2-C7	1.436(2)	C3-C4	1.359(2)
C4-C5	1.416(2)	C5-C6	1.349(2)
C6-C7	1.426(2)	C7-C8	1.390(2)
C8-C9	1.391(2)	C9-C10	1.424(2)
C9-C14	1.436(2)	C10-C11	1.349(3)
C11-C12	1.415(2)	C12-C13	1.361(2)
C13-C14	1.419(2)	C15-C15	1.202(3)

Table 5. Bond angles (°) for 1α.

C2-C1-C14	120.04(14)	C2-C1-C15	120.00(15)
C14-C1-C15	119.96(15)	C1-C2-C3	122.57(15)
C1-C2-C7	119.62(16)	C3-C2-C7	117.80(15)
C4-C3-C2	121.37(16)	C3-C4-C5	120.68(18)
C6-C5-C4	120.09(17)	C5-C6-C7	121.20(16)
C8-C7-C6	121.72(16)	C8-C7-C2	119.44(16)
C6-C7-C2	118.84(16)	C7-C8-C9	121.98(15)
C8-C9-C10	121.62(15)	C8-C9-C14	119.47(16)
C10-C9-C14	118.91(16)	C11-C10-C9	121.23(17)
C10-C11-C12	120.22(18)	C13-C12-C11	120.46(18)
C12-C13-C14	121.50(16)	C13-C14-C1	122.89(15)
C13-C14-C9	117.68(16)	C1-C14-C9	119.42(15)
C15-C15-C1	179.6(2)		

Table 6. Anisotropic atomic displacement parameters (Å²) for 1α.

The anisotropic atomic displacement factor exponent takes the form: $-2\pi^2[h^2 a^{*2} U_{11} + ... + 2 h k a^* b^* U_{12}]$

	U_{11}	U_{22}	U_{33}	U_{23}	U_{13}	U_{12}
C1	0.0425(10)	0.0305(8)	0.0328(8)	0.0011(6)	-0.0050(7)	0.0022(7)
C2	0.0442(10)	0.0325(8)	0.0341(9)	0.0011(7)	-0.0059(7)	0.0041(7)
C3	0.0518(12)	0.0412(9)	0.0427(10)	-0.0041(7)	-0.0006(8)	-0.0019(8)
C4	0.0520(12)	0.0569(11)	0.0466(11)	-0.0029(8)	0.0052(9)	0.0003(9)
C5	0.0559(12)	0.0550(11)	0.0442(11)	-0.0092(8)	0.0027(9)	0.0126(9)
C6	0.0552(12)	0.0420(9)	0.0435(10)	-0.0089(7)	-0.0045(9)	0.0078(8)
C7	0.0492(10)	0.0337(8)	0.0356(9)	-0.0001(7)	-0.0071(7)	0.0073(7)
C8	0.0521(11)	0.0357(9)	0.0398(10)	-0.0040(7)	-0.0105(8)	0.0001(8)
C9	0.0460(10)	0.0343(8)	0.0389(9)	0.0039(7)	-0.0095(8)	-0.0003(7)
C10	0.0515(11)	0.0439(9)	0.0471(10)	0.0034(8)	-0.0086(9)	-0.0072(8)
C11	0.0468(11)	0.0575(11)	0.0532(12)	0.0102(9)	-0.0028(9)	-0.0076(9)
C12	0.0558(12)	0.0561(11)	0.0461(10)	0.0021(8)	0.0045(9)	-0.0013(9)
C13	0.0527(12)	0.0449(9)	0.0396(10)	-0.0017(7)	-0.0001(8)	-0.0027(8)
C14	0.0447(10)	0.0322(8)	0.0354(9)	0.0034(7)	-0.0060(7)	0.0021(7)
C15	0.0435(10)	0.0376(8)	0.0346(9)	0.0009(6)	0.0011(7)	0.0017(7)

Table 7. Hydrogen atomic coordinates and isotropic atomic displacement parameters (Å²) for 1α.

	x/a	y/b	z/c	U(eq)
H3	1.1190	0.3735	0.3588	0.054
H4	1.2023	0.2300	0.2371	0.062
H5	1.1290	-0.1220	0.1498	0.062
H6	0.9713	-0.3202	0.1842	0.057
H8	0.8176	-0.3469	0.2781	0.052
H10	0.6604	-0.3729	0.3679	0.058
H11	0.5683	-0.2246	0.4839	0.063
H12	0.6390	0.1232	0.5745	0.063
H13	0.8014	0.3152	0.5482	0.055

Table 8. Sample and crystal data for 1β.

Identification code	RRCDt1465 CCDC **1036772**
Chemical formula	$C_{30}H_{18}$
Formula weight	378.44 g/mol
Temperature	273(2) K
Wavelength	0.71073 Å
Crystal size	0.100 x 0.150 x 0.180 mm
Crystal system	monoclinic
Space group	C 1 2/c 1
Unit cell dimensions	a = 12.8185(10) Å α = 90°
	b = 14.0656(11) Å β = 112.1330(10)°
	c = 11.5956(9) Å γ = 90°
Volume	1936.6(3) $Å^3$
Z	4
Density (calculated)	1.298 g/cm^3
Absorption coefficient	0.074 mm^{-1}
F(000)	792

Table 9. Data collection and structure refinement for 1β.

Theta range for data collection	2.25 to 27.12°
Index ranges	-15<=h<=16, -18<=k<=16, -14<=l<=14
Reflections collected	8566
Independent reflections	2147 [R(int) = 0.0181]
Coverage of independent reflections	100.0%
Absorption correction	multi-scan
Max. and min. transmission	0.9930 and 0.9870
Refinement method	Full-matrix least-squares on F^2
Refinement program	SHELXL-2014/6 (Sheldrick, 2014)
Function minimized	$\Sigma\, w(F_o^2 - F_c^2)^2$
Data / restraints / parameters	2147 / 0 / 136
Goodness-of-fit on F^2	1.060
Final R indices	1636 data; I>2σ(I) R1 = 0.0485, wR2 = 0.1391
	all data R1 = 0.0611, wR2 = 0.1530
Weighting scheme	$w=1/[\sigma^2(F_o^2)+(0.0941P)^2+0.2717P]$ where $P=(F_o^2+2F_c^2)/3$
Largest diff. peak and hole	0.259 and -0.179 $eÅ^{-3}$
R.M.S. deviation from mean	0.043 $eÅ^{-3}$

Table 10. Atomic coordinates and equivalent isotropic atomic displacement parameters (Å²) for 1β.

U(eq) is defined as one third of the trace of the orthogonalized U_{ij} tensor.

	x/a	y/b	z/c	U(eq)
C1	0.33263(9)	0.36107(8)	0.64260(10)	0.0310(3)
C2	0.28284(9)	0.43374(9)	0.55494(10)	0.0332(3)
C3	0.34715(11)	0.50577(9)	0.52597(11)	0.0409(3)
C4	0.29590(13)	0.57574(11)	0.44239(13)	0.0513(4)
C5	0.17662(14)	0.57868(12)	0.38304(13)	0.0576(4)
C6	0.11289(12)	0.51058(11)	0.40689(12)	0.0504(4)
C7	0.16232(10)	0.43498(9)	0.49170(11)	0.0384(3)
C8	0.09799(10)	0.36361(10)	0.51610(11)	0.0416(3)
C9	0.14645(10)	0.28944(9)	0.59840(11)	0.0378(3)
C10	0.08112(11)	0.21557(11)	0.62361(13)	0.0499(4)
C11	0.13066(13)	0.14504(11)	0.70485(14)	0.0555(4)
C12	0.24891(13)	0.14225(11)	0.76680(13)	0.0507(4)
C13	0.31445(11)	0.21114(9)	0.74657(11)	0.0415(3)
C14	0.26642(9)	0.28732(8)	0.66292(10)	0.0330(3)
C15	0.45140(9)	0.36287(8)	0.71589(10)	0.0331(3)

Table 11. Bond lengths (Å) for 1β.

C1-C2	1.4129(16)	C1-C14	1.4152(16)
C1-C15	1.4373(14)	C2-C3	1.4239(18)
C2-C7	1.4391(16)	C3-C4	1.3638(19)
C3-H3	0.93	C4-C5	1.421(2)
C4-H4	0.93	C5-C6	1.353(2)
C5-H5	0.93	C6-C7	1.4247(19)
C6-H6	0.93	C7-C8	1.3941(19)
C8-C9	1.3922(19)	C8-H8	0.93
C9-C10	1.4320(18)	C9-C14	1.4348(16)
C10-C11	1.351(2)	C10-H10	0.93
C11-C12	1.412(2)	C11-H11	0.93
C12-C13	1.3595(19)	C12-H12	0.93
C13-C14	1.4205(17)	C13-H13	0.93
C15-C15	1.198(2)		

Table 12. Bond angles (°) for 1β.

C2-C1-C14	120.89(10)	C2-C1-C15	120.22(10)
C14-C1-C15	118.85(10)	C1-C2-C3	122.66(10)
C1-C2-C7	118.86(11)	C3-C2-C7	118.48(11)
C4-C3-C2	120.96(12)	C4-C3-H3	119.5
C2-C3-H3	119.5	C3-C4-C5	120.49(14)
C3-C4-H4	119.8	C5-C4-H4	119.8
C6-C5-C4	120.17(13)	C6-C5-H5	119.9
C4-C5-H5	119.9	C5-C6-C7	121.57(12)
C5-C6-H6	119.2	C7-C6-H6	119.2
C8-C7-C6	122.30(11)	C8-C7-C2	119.43(11)
C6-C7-C2	118.27(12)	C9-C8-C7	122.24(10)
C9-C8-H8	118.9	C7-C8-H8	118.9
C8-C9-C10	122.65(11)	C8-C9-C14	119.13(11)
C10-C9-C14	118.21(12)	C11-C10-C9	121.20(12)
C11-C10-H10	119.4	C9-C10-H10	119.4
C10-C11-C12	120.50(13)	C10-C11-H11	119.7
C12-C11-H11	119.7	C13-C12-C11	120.47(14)
C13-C12-H12	119.8	C11-C12-H12	119.8
C12-C13-C14	121.22(12)	C12-C13-H13	119.4
C14-C13-H13	119.4	C1-C14-C13	122.26(10)
C1-C14-C9	119.35(11)	C13-C14-C9	118.39(11)
C15-C15-C1	175.39(16)		

Table 13. Anisotropic atomic displacement parameters (Å²) for 1β.

The anisotropic atomic displacement factor exponent takes the form: $-2\pi^2[h^2 a^{*2} U_{11} + ... + 2 h k a^* b^* U_{12}]$

	U_{11}	U_{22}	U_{33}	U_{23}	U_{13}	U_{12}
C1	0.0249(5)	0.0381(7)	0.0280(5)	-0.0043(4)	0.0077(4)	0.0003(4)
C2	0.0299(6)	0.0396(7)	0.0279(6)	-0.0047(4)	0.0083(5)	0.0022(4)
C3	0.0404(7)	0.0453(8)	0.0349(6)	-0.0013(5)	0.0118(5)	-0.0003(5)
C4	0.0631(9)	0.0480(8)	0.0418(7)	0.0061(6)	0.0186(7)	0.0006(6)
C5	0.0680(10)	0.0576(9)	0.0391(8)	0.0119(6)	0.0111(7)	0.0196(7)
C6	0.0421(7)	0.0652(10)	0.0344(7)	0.0013(6)	0.0035(6)	0.0162(6)
C7	0.0313(6)	0.0496(8)	0.0288(6)	-0.0050(5)	0.0053(5)	0.0071(5)
C8	0.0229(6)	0.0612(9)	0.0346(6)	-0.0111(6)	0.0038(5)	0.0009(5)
C9	0.0291(6)	0.0513(8)	0.0324(6)	-0.0106(5)	0.0109(5)	-0.0054(5)
C10	0.0346(7)	0.0706(10)	0.0456(8)	-0.0152(7)	0.0162(6)	-0.0171(6)
C11	0.0563(9)	0.0643(10)	0.0510(8)	-0.0066(7)	0.0262(7)	-0.0246(7)
C12	0.0584(8)	0.0501(8)	0.0443(8)	0.0029(6)	0.0200(6)	-0.0084(6)
C13	0.0385(7)	0.0473(8)	0.0372(7)	0.0002(5)	0.0127(5)	-0.0030(5)
C14	0.0285(6)	0.0418(7)	0.0281(6)	-0.0061(5)	0.0099(5)	-0.0021(5)
C15	0.0286(5)	0.0368(7)	0.0326(6)	-0.0002(4)	0.0100(4)	0.0002(4)

Table 14. Hydrogen atomic coordinates and isotropic atomic displacement parameters (Å²) for 1β.

	x/a	y/b	z/c	U(eq)
H3	0.4252	0.5051	0.5646	0.049
H4	0.3393	0.6219	0.4241	0.062
H5	0.1423	0.6275	0.3277	0.069
H6	0.0350	0.5132	0.3670	0.06
H8	0.0201	0.3656	0.4760	0.05
H10	0.0032	0.2162	0.5833	0.06
H11	0.0866	0.0979	0.7201	0.067
H12	0.2822	0.0929	0.8218	0.061
H13	0.3922	0.2083	0.7883	0.05

Complete computational details and discussions

Isolated molecule "gas-phase" conformation analysis

Gas-phase conformational analysis of **1** was carried out at PBE0/6-31G(d,p) level using Gaussian03 (G03). Tight convergence criteria and ultrafine integral grid were used to ensure proper convergence. Starting from molecular conformations in DITBEN and **1β**, optimizations lead to two distinct stationary points on the potential energy surface, one with ring-ring torsion angle τ=-1.75°, obtained from DITBEN and another with τ=35.60°, from the new form. The stationary point obtained from DITBEN turned out to be a transition state (energy maximum) with one imaginary frequency at -18.3 cm^{-1}, whose corresponding displacement vector tends to twist the two anthryl rings away from being parallel. The gas-phase energy difference between the maximum and the minimum at this level was 6.48 kJ/mol (5.84 kJ/mol with zero-point energy (ZPE) correction). The gas-phase optimized planar conformer also correctly reproduces the small steps between the two anthryl rings. In contrast, τ in the optimized twisted conformer has deviated significantly from its value in the **1β** crystal. Obviously packing force played noticeable role in determining the conformation of the component molecule in its crystal.

Starting with the optimized stationary point shown in DITBEN, the potential energy curve in Figure 4 in the main article was obtained by scanning the torsion angle τ in 20° steps. In each step, all the other degrees of freedom in the molecule were allowed to be relaxed. Similar conformational analysis and potential energy scan were also repeated with pure PBE functional in G03, to give us some indications of the underlying conformational energetics in CASTEP calculations. The obtained potential energy curve is shown as the dash-dot line in Figure 4 in the main article. In this case two similar stationary points were located at τ=-1.78° and 31.37°. The energy difference between them is 4.97 kJ/mol (4.26 kJ/mol with ZPE correction). The heights of the two potential barriers on the potential energy curve have changed, with the one at 90° become higher than the one at near planarity. This, combined with the lower energy of the planar conformations, leads to an interesting observation that the intramolecular energy of the molecular conformation at the τ values observed in the new form, labelled as the yellow lines in Figure 4 in the main article, now lies almost within 1kJ/mol of the intramolecular energy of the planar conformer. This means that at PBE/6-31G(d,p) level the two conformations are competitive in terms of intramolecular energy. The B3LYP/6-311+G(d,p) results in the literature[1] give a much lower energy difference with the planar (0°) only 0.4 kcal/mol (1.7kJ/mol) higher in energy than a twisted conformation found at 38.2°. Thus there is considerable difference in the quantum mechanical estimates of the intramolecular conformational differences, which is understandable given the quality of the practically feasible calculations[2], but the planar conformation in DITBEN is clearly less stable than that in **1β**, with the best estimate being with the PBE0 functional of 4 kJ mol^{-1}.

Note the four atoms in the acetylene group (C_1, C_{15}, C_{15a} and C_{1a}) in **1** are not exactly collinear, hence two values of τ can be obtained by measuring either side of the molecule.

CASTEP calculations on crystal

Conventional DFT calculations are known to have difficulty with noncovalent interactions, such as those existing in aromatic π-stacking. Therefore, several dispersion corrected schemes have been put forward as remedies, known generically as DFT+D. Variable cell DFT+D optimizations of the two forms of **1** were carried out using pure PBE exchange-

correlation functional and two different dispersion correction schemes, Tkatchenko-Scheffler's scheme (TS) and Grimme's scheme (G06), henceforth called PBE+TS and PBE+G06 calculations respectively. Both methods were used as we have previously observed, the choice of dispersion correction can make a significant difference to the relative lattice energies[3] and [4]. CASTEP version 7.0.2 was used for all the calculations. Monkhurst-Pack *k* points were automatically generated and used in all the calculations. Plane wave cutoff energies and k-points were tested for convergence before their values were chosen as shown in Figure 1. This led to the use of a cutoff energy of 700 eV and k-point spacing set of 0.04 $Å^{-1}$, which corresponds to 9 sampling k-points in the reciprocal space. On-the-fly ultrasoft pseudopotentials were also used. Once an optimization has converged, a single-point calculation at the resultant structure was carried out to examine the effect of changing cell parameters on the k-points.

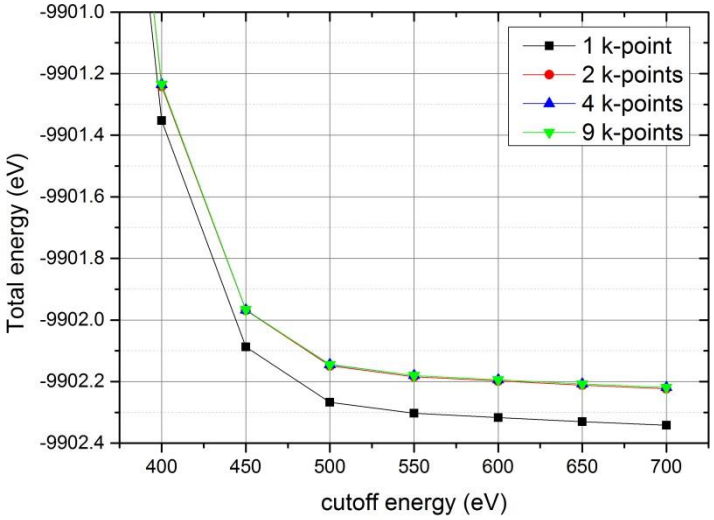

Figure 1 Convergence test of single point total energy of DITBEN structure for plane wave cutoff energies and k-point sampling used in the optimizations. Note that the values for 2, 4 and 9 k-points are superimposed.

Experimental structures of DITBEN and **1β** were converted to P1 group with *cif2cell*, which were then used as the initial structures in the optimizations. The optimized cell parameters and other results were shown in Table 15.

Table 15 DFT+D optimized lattice parameters of the two forms of 1, compared to experimental values.

	a (Å)	b (Å)	c (Å)	α (°)	β (°)	γ (°)	Cell Vol. ($Å^3$)	$RMSD_{15}$ (Å)
Form 1α								
PBE+TS opt	12.1441	5.0412	18.2934	90.000	125.972	90.000	906.365	0.187
PBE+G06 opt	12.0392	5.0331	18.2299	90.000	126.406	90.000	889.049	0.245
DITBEN exp.	12.432	5.112	18.758	90.000	126.58	90.000	957.299	-
Form 1β								
PBE+TS opt	12.4884	13.9127	11.4469	90.000	110.634	90.000	1861.28	0.202
PBE+G06 opt	12.5066	14.0427	10.8972	90.000	109.860	90.000	1800.01	0.411
Form 1β exp.	12.8183	14.0649	11.5954	90.000	112.132	90.000	1936.48	-

As shown by $RMSD_{15}$ values, obtained through a comparison of 15-molecule clusters in experimental and optimized crystal structures, in both forms of **1**, the TS scheme was able to reproduce the overall packing better than the G06 scheme, as has been generally

observed [5]. Overlays between PBE+TS optimized and experimentally observed structures are shown in Figure 2.

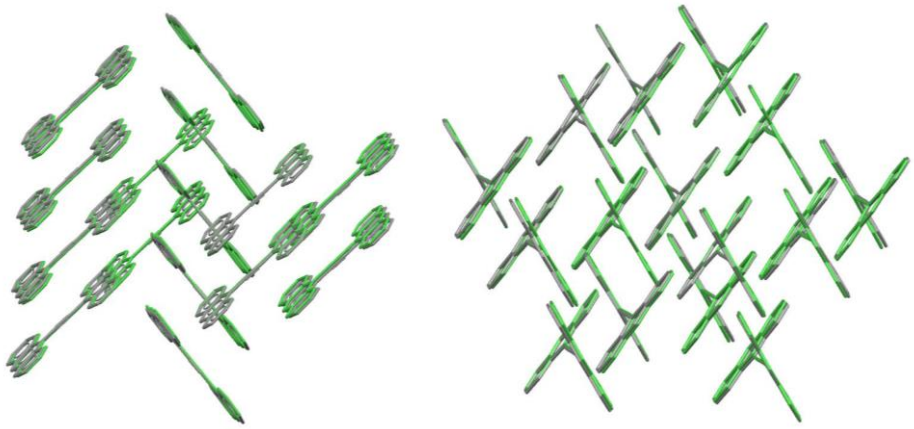

Figure 2 Overlay of PBE+TS optimized crystal structures with experimentally observed DITBEN (left) and 1β (right) structures. Experimental structures are in green. Hydrogen atoms have been ignored for clarity.

Table 16 is a comparison of molecular conformations obtained in the optimized structures with those in the experimental crystal structures. The $RMSD_1$ and MaxD values show how well the experimentally observed molecular conformations were reproduced after the optimizations. Both dispersion correction schemes worked well in this case, again with the TS scheme performing slightly better. The optimized structures reproduce the deviation from linearity of the four atoms forming the acetylene bridge between the two rings in **1** in the optimized **1β** structure, in contrast to the gas-phase optimized geometry. The values of the bond angles of the C≡C triple bonds ($\angle C_1\text{-}C_{15}\text{-}C_{15a}$ and $\angle C_{15}\text{-}C_{15a}\text{-}C_{1a}$) which are linear (180°) in the gas phase, are shown in Table 16 to agree very well with the experimental values, indicating that the optimizations were capable of capturing the fine details of intermolecular interactions. The breakdown of linearity of the four atoms also leads to two values for τ for the twisted forms and again their optimized values agree perfectly with those observed in experimental **1β** form.

Table 16 Comparison of molecular conformations between experimental and DFT+D optimized structures.

	τ (°)	$\angle C_1\text{-}C_{15}\text{-}C_{15a}$ (°)	$RMSD_1$ (Å)	MaxD (Å)
Form 1α				
PBE+TS opt	-0.79	179.49	0.0227	0.0396
PBE+G06 opt	-0.77	179.20	0.0288	0.0502
DITBEN exp.	1.02	178.82	-	-
Form 1β				
PBE+TS opt	61.58, 67.41	174.30	0.0539	0.1074
PBE+G06 opt	59.76, 65.55	175.55	0.0728	0.1222
Form 1β exp.	63.31, 68.89	175.37	-	-

The relative total energies of the two optimized forms at different levels were listed in Table 16 and shown in Figure 3, along with those obtained through rigid-molecule optimizations with DMACRYS (ExpMinExp), which will be discussed later. In all methods used in this study, the DITBEN structure, formed with planar molecules of **1**, is found to be more stable than the new form. This is so despite the fact that all gas-phase conformation analysis, in the current study or in the literature, showed that the planar structure

corresponds to a higher-energy transition state and the global minimum is in a twisted conformation.

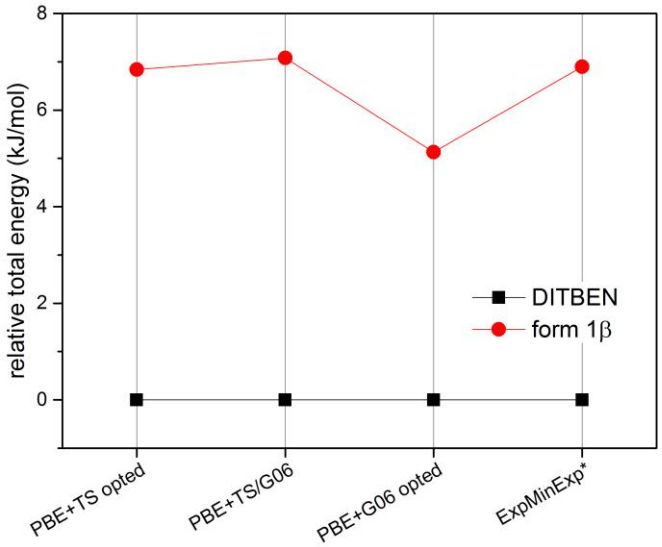

Figure 3 Comparison of relative energies between DITBEN and form 1β, obtained with various theoretical levels.

Table 17 Predicted relative stability of the two forms of 1, the energy of DITBEN was chosen as zero.

	Relative total energy (kJ/mol)	
	Form 1α (DITBEN)	**Form 1β**
CASTEP		
PBE+TS opt	0.00	6.84
PBE+TS/G06	0.00	7.09
PBE+G06 opt	0.00	5.13
DMACRYS		
ExpMinExp	0.00	~ 6.9 (ΔU_{inter}=10.93)

*** DMACRYS results used an estimated ΔE_{intra} ~ -4.0 kJ/mol for form 1β, obtained from Figure 4 in the main article.**

DMACRYS (ExpMinExp) calculations

Instead of calculating the lattice energy from first principle using DFT+D methods, another well-established approach for obtaining lattice energy is based on writing E_{latt} as the sum of an intermolecular interaction energy U_{inter} and an intramolecular part ΔE_{intra} :

$$E_{latt} = U_{inter} + \Delta E_{intra}.$$

ΔE_{intra} can be obtained from *ab initio* calculations, while U_{inter} is calculated by summing over various contributing intermolecular interactions, which include electrostatic, induction, dispersion and exchange-repulsion interactions. The electrostatic interactions were calculated from distributed atomic multipoles to account for the anisotropic nature of electron lone pairs and hydrogen bonds. Dispersion and exchange-repulsion interactions are evaluated from an exp-6 potential with empirically fitted (FIT) potential parameters. Rigid molecular conformations were used in these calculations using DMACRYS. As the conformations come from experimentally observed structures, they are denoted as ExpMinExp. For the current calculations, DMACRYS version 2.0.8 was used and PBE0/6-31G(d,p) wavefunctions were used to calculate the distributed multipoles. Between the two crystal forms, DITBEN was found to be able to pack more efficiently, with a ΔU_{inter} = 10.93 kJ/mol. Adding to it the estimated difference in intramolecular energies (4.0 kJ mol^{-1} from

Figure in the main article), DITBEN was again found to be the form with a lower lattice energy by 6.9 kJ/mol, as shown in Table 18.

Table 18 DMACRYS optimized lattice parameters using rigid molecule conformations from experimental structures.

	a (Å)	b (Å)	c (Å)	α (°)	β (°)	γ (°)	Cell Vol. (Å^3)	RMSD$_{15}$ (Å)
Form 1α								
ExpMinExp	12.5030	4.9986	18.9062	90.000	125.849	90.000	957.752	0.182
DITBEN exp.	12.432	5.112	18.758	90.000	126.58	90.000	957.299	-
Form 1β								
ExpMinExp	12.7454	14.4406	11.6001	90.000	111.374	90.000	1988.16	0.148
Form 1β exp.	12.8183	14.0649	11.5954	90.000	112.132	90.000	1936.48	-

As shown in Table 18, given the conformations adopted by **1** in the two crystal structures, DMACRYS reproduced the experimental structures very well. Energetically as shown in Table 19, DMACRYS results showed that DITBEN form can pack more efficiently, leading to stronger intermolecular interactions. As expected, dispersion interaction dominates the intermolecular interaction in both forms, while total electrostatic interaction contributes very little and is of similar size in both forms. Thus it can be concluded that the stability of DITBEN comes from its capability for better van der Waals packing of the molecules. Although this may be attributed to better π-π stacking, just the greater density of DITBEN compared with **1β** would be expected to give a lower lattice energy, and more favorable dispersion interactions.

Table 19 Decomposition of intermolecular energies in forms 1α and 1β.

ExpMinExp	U_{inter} (kJ/mol)	$U_{rep\text{-}dis}$ (kJ/mol)	U_{es} (kJ/mol)
Form 1α	-197.6399	-191.1078	-6.5320
Form 1β	-186.7088	-180.3407	-6.3681
$\Delta E_{1\beta\text{-}1\alpha}$	10.9311	10.7671	0.1639

Morphology calculations

The morphologies in Figures 1(c) and 2(c) in the main article were generated using the BFDH model in Mercury, and the crystal structures were redefined to have an entire molecule in the unit cell.

The morphologies were also calculated using attachment energy model[6] [7], using ExpMinExp structures (again using a Z'=1 definition), the FIT potential and the potential derived charges of the PBE0/6-31G(d,p) wavefunctions. Taking into account the strength of the intermolecular forces does not change the gross predicted morphology of the crystals, though some small faces differ. The relative volume growth rates of the two forms by sublimation are estimated at 1:0.9 for **1α:1β.**

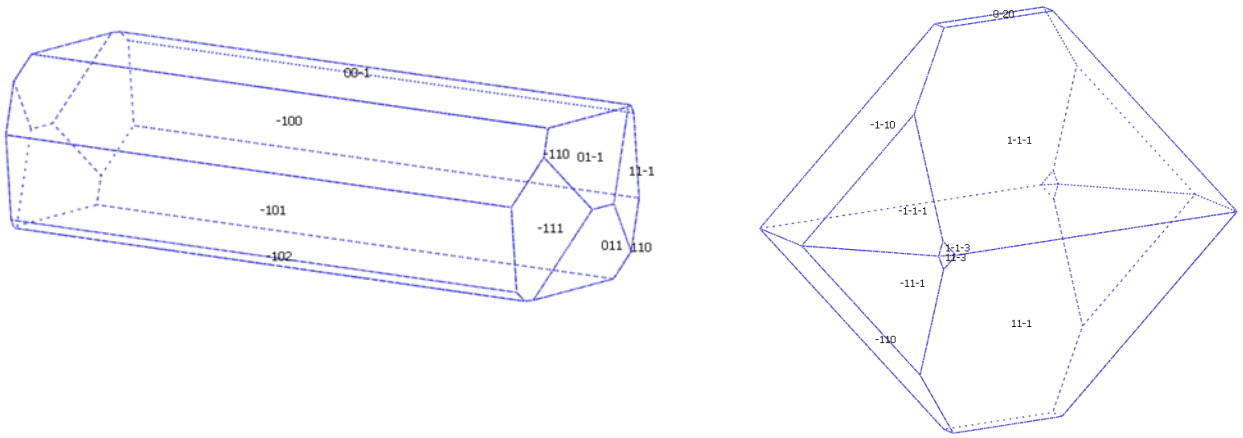

Figure 4 The attachment energy predicted morphologies of 1α (left) and 1β (right).

References

1. Gutierrez-Arzaluz, L.; Guarin, C. A.; Rodriguez-Cordoba, W.; Peon, J., Dynamics of the Formation of a Charge Transfer State in 1,2-Bis(9-anthryl)acetylene in Polar Solvents: Symmetry Reduction with the Participation of an Intramolecular Torsional Coordinate. *Journal of Physical Chemistry B* **2013,** *117* (40), 12175-12183.
2. van Mourik, T.; Karamertzanis, P. G.; Price, S. L., Molecular conformations and relative stabilities can be as demanding of the electronic structure method as intermolecular calculations. *Journal of Physical Chemistry A* **2006,** *110* (1), 8-12.
3. Gelbrich, T.; Braun, D. E.; Ellern, A.; Griesser, U. J., Four Polymorphs of Methyl Paraben: Structural Relationships and Relative Energy Differences. *Crystal Growth & Design* **2013,** *13* (3), 1206-1217.
4. Braun, D. E.; McMahon, J. A.; Koztecki, L. H.; Price, S. L.; Reutzel-Edens, S. M., Contrasting Polymorphism of Related Small Molecule Drugs Correlated and Guided by the Computed Crystal Energy Landscape. *Crystal Growth & Design* **2014,** *14* (4), 2056-2072.
5. Binns, J.; Healy, M. R.; Parsons, S.; Morrison, C. A., Assessing the performance of density functional theory in optimizing molecular crystal structure parameters. *Acta Crystallographica Section B-Structural Science Crystal Engineering and Materials* **2014,** *70*, 259-267.
6. Hartman, P.; Perdok, W. G., On the Relations Between Structure and Morphology of Crystals. I. *Acta Crystallographica* **1955,** *8* (1), 49-52.
7. Hartman, P.; Bennema, P., The Attachemnt Energy as a Habit Controlling Factor 1. Theoretical Considerations. *Journal of Crystal Growth* **1980,** *49* (1), 145-156.